Characterization of the 1117-meV and 1052-meV optical transitions in heat-treated Si

L. Jeyanathan,* Gordon Davies, and E. C. Lightowlers
Physics Department, King's College London, Strand, London WC2R 2LS, United Kingdom
(Received 14 April 1995)

Four conflicting models have been proposed for the origin of the O^j and $O^{j'}$ photoluminescence transitions that are observed near 1117 and 1052 meV in heat-treated, oxygen-rich silicon. To distinguish between them we have investigated the effects on the optical transitions of magnetic and stress perturbations. We show that both the O^j and the $O^{j'}$ lines are produced by recombination of excitons bound to isoelectronic centers of rhombic I (C_{2v}) symmetry. The excitons have an electron derived from a pair of conduction-band minima and a hole in an orbital singlet state. The electronic states and the symmetry are reminescent of the thermal donors in silicon, supporting the suggestion that the O^j and $O^{j'}$ centers may have evolved from them. There is clear evidence that both centers may trap one or two excitons, accounting for most of the luminescence structure, but the specific origin of one exciton-related weak line at both O^j and $O^{j'}$ remains uncertain.

I. INTRODUCTION

Many crystalline defects are generated in Czochralski-grown (oxygen-rich) silicon when it is heated between 450 and 500 °C. It is well known that during this annealing the oxygen atoms become mobile and aggregate. One important group of defects which is created is the electrically active thermal-donor complexes, whose microscopic structure is still uncertain.[1] Other chemical reactions are also triggered by the aggregation. Each pair of O atoms which aggregate releases one self-interstitial.[2] The self-interstitial may combine with a substitutional carbon atom to produce a split-interstitial carbon atom which in turn may aggregate with another impurity.[3] Some of these processes are illustrated by Fig. 1, which shows the evolution of the luminescence spectrum of boron-doped, oxygen-rich silicon after heating at 450° for various times. The figure shows the loss, in the first tens of hours, of luminescence (labeled *B*) from the boron acceptors, as the boron is displaced from the substitutional sites.[4] The growth and then destruction of luminescence (labeled TD) ascribed to thermal donors[5] occurs during the first 100 h, and within this time the *P* line, which is probably produced by a carbon interstitial trapped at a pair of oxygen atoms,[6] is also produced and then destroyed.

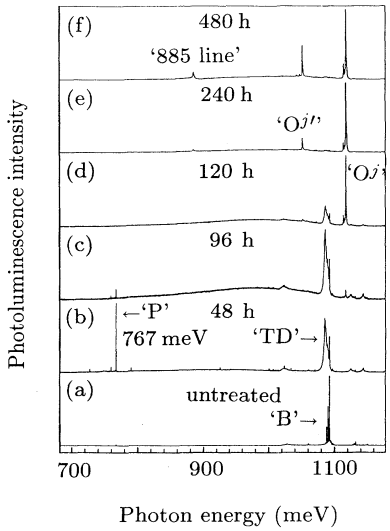

FIG. 1. Photoluminescence spectra measured at 4.2 K showing the growth of the O^j and $O^{j'}$ systems with increasing annealing time at 450 °C of an initially *p*-type, oxygen-rich, carbon-lean Cz sample. (a) Untreated. (b) 48 h. (c) 96 h. (d) 120 h. (e) 240 h. (f) 480 h. The spectra have been normalized to the same maximum peak height and for clarity are displaced vertically. *B* and TD label the decay of an exciton bound to a neutral boron acceptor or a thermal donor, respectively, with the emission of one transverse-optic wave-vector-conserving phonon. *P* is the zero-phonon line of a carbon-oxygen complex.

This paper is concerned with the two defect systems which produce the multiple zero-phonon lines near 1117 meV (labeled O^j on Fig. 1) and 1052 meV ($O^{j'}$, Fig. 1). The lines are shown in more detail in Fig. 2. To avoid confusion from the different labeling systems adopted by different workers, the nomenclature of Thewalt *et al.*[7] and Steele, Thewalt, and Watkins[8] will be used throughout this paper. The O^j and $O^{j'}$ systems are produced after annealing for a few hundred hours at these temperatures, and are then destroyed at longer times.[9] To date, four different physical processes have been proposed to describe the origin of these systems. Weber and Queisser[10] interpreted the O^j lines as being due to transitions between free holes and electrons bound to different thermal donors, on the basis of the asymmetric line shapes (which can be seen in Fig. 2). In further support of the model they also noted that the transition energies were consistent with the known ionization energies of several neutral thermal donors. The $O^{j'}$ system, observed as a single line, was ascribed by them to a zone-center optical-phonon replica of the strongest O^j line; however, we note immediately that the different intensity ratios of O^j and $O^{j'}$ in Figs. 1(d)–1(f) show that they occur at

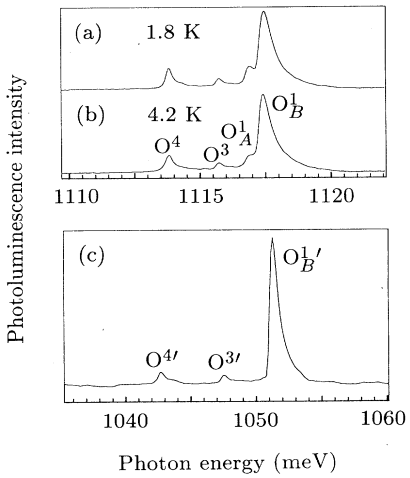

FIG. 2. Photoluminescence spectra of the O^j system, obtained with the sample in a bath at (a) ~1.8 K and (b) 4.2 K, using a laser excitation of 200 mW which produces some heating. The sample had been annealed at 450 °C for 120 h. The intensity of the O^1_A line increases relative to that of the O^1_B line with decreasing temperature. (c) The $O^{j'}$ system recorded at 4.2 K with 200-mW laser excitation using a sample which had been annealed for 480 h. In normal conditions there is no detectable $O^{1'}_A$ line, but it can be induced by a magnetic-field perturbation. Note that the energy scale of (c) is double that of (a) and (b).

different defects. Later, Weber *et al.*[11] suggested that the main transition, O^1, could be a recombination of a free hole with an electron at a "new" oxygen precipitate, while retaining the free-hole to thermal-donor interpretation for the other lines.

Dörnen and Hangleiter[12] observed that luminescence from the $O^{1'}$ line has a significantly shorter decay time than that from O^1, establishing that $O^{1'}$ is not a phonon replica of O^1. They also showed that the intensities of all the lines decay nonexponentially with time. They suggested that the O^j lines were due to donor-acceptor pair recombinations involving neutral thermal donors and boron acceptors, and that the $O^{j'}$ lines were donor-acceptor pair spectra involving singly ionized thermal donors and boron acceptors.

An entirely different model was proposed by Thewalt *et al.*[7] They reported luminescence excitation measurements, which established that the asymmetric line shapes were caused by inhomogeneous broadening of the transitions. Comparison with the earlier work of Dörnen and Hangleiter[12] implies that the luminescence from the highly perturbed centers producing the long tail of the O^1 line has a shorter lifetime than from the less-perturbed centers; the variation would cause nonexponential decays of the luminescence, and will be referred to again in Sec. V. Thewalt *et al.*[7] interpreted the main O^1 line, with its long radiative lifetime of up to 85 μs at 1.6 K, as the decay of an exciton bound to an isoelectronic center. The much faster decaying O^3 and O^4 transitions (initial lifetimes, immediately after excitation, of 33 and 8 ns at 4.2 K) were assigned to the decay of the third and fourth excitons bound at the same center. The second bound multiexciton line was thought to lie beneath O^1, since the spectral region also has a component which decays rapidly. A very similar interpretation was given to the origin of the $O^{j'}$ lines.[8] Thewalt *et al.*[7] observed that energy could be transferred from an exciton bound to a neutral P donor to the O^j center; intercenter transfer could be another source of nonexponential decays. They also reported a series of excited states of the O^j center, lying between 12 and 30 meV above the O^1 excited state.

Recently, Liesert, Gregorkiewicz, and Ammerlaan[9] suggested that the O^j and $O^{j'}$ lines are caused by the decay of an exciton bound to a thermal donor, with the internal excitation of an electron at the donor (a two-electron transition).

Further experimental data are required to distinguish between these different models. In this paper we report the effects of perturbations on the optical spectra. We show in Sec. III that magnetic fields perturb the O^1 and $O^{1'}$ lines and induce nearby transitions in a way consistent with an exciton being bound to an isoelectronic center, with the hole being the relatively tightly bound particle. In Secs. IV and V we show that uniaxial stresses perturb primarily the electron component of the excitons, and we establish that the electron is a conduction-band-like particle derived from a pair of conduction-band minima. The symmetry of both the O^j and $O^{j'}$ defects is shown to be rhombic I. The electronic structure, the defect symmetries, and the production of the defects suggest that they are the evolution products of the thermal donors after further annealing. The changes in the spectra under increasing excitation and stress indicate that the O^4 and $O^{4'}$ lines are produced by the decay of a second exciton bound to the complexes. Our data thus support the proposal by Thewalt *et al.*[7] that the O^j and $O^{j'}$ features occur at isoelectronic centers, which are produced from the thermal donors. The paper begins by describing the experimental techniques used here.

II. EXPERIMENTAL DETAILS

The material used in the investigation was carbon-lean p-type Czochralski (CZ) Si, ~30–50 Ω cm. The samples were etched in 10% HF in HNO_3 and RCA cleaned before all heat treatments. They were annealed at 450 °C in a flowing Ar atmosphere for various times up to 480 h in RCA-cleaned quartz tube. Uniaxial stress measurements were made at 4.2 K, with the samples immersed in liquid helium. The stress measurements were carried out on x-ray-oriented $12\times4\times2$-mm^3 samples with the long axis in a $\langle 001\rangle$, $\langle 111\rangle$, or $\langle 110\rangle$ direction. Polarization studies were carried out with the laser excitation normal to the back 12×4-mm^2 plane, and the photoluminescence detected normal to the front 12×4-mm^2 plane. To reduce the loss of polarization in the signal by reflection and refraction, the corners of the samples were painted with colloidal graphite. The Zeeman experiments were carried out with a magnetic field up to 6 T, applied in turn along the three principal crystallographic directions in an Oxford instruments drip feed cryostat fitted with a

Helmholtz pair of superconducting coils. The luminescence was excited by 514.5-nm Ar^+ laser, and the spectra were recorded either using a Nicolet 60SX or a Bomem DA8 Fourier-transform spectrometer fitted with liquid-N_2-cooled North Coast germanium diode detectors.

III. MAGNETIC-FIELD PERTURBATION STUDIES

The effects on the O^j and $O^{j'}$ systems have been measured for magnetic fields up to 5.5 T applied along the ⟨001⟩, ⟨111⟩, and ⟨110⟩ crystal axes. For both systems the O_B^1, O^3, and O^4 lines are not perturbed within the resolution available, which is limited to 0.6 meV by the inhomogeneous line broadening. However, the O_A^1 line splits into two observable components with relative intensities which follow a Boltzmann relationship characterized by an energy equal to the observed splittings (Fig. 3). The splitting is the same for all directions of the magnetic field, and has the magnitude shown in Fig. 4(a). Very similar data are obtained for the $O^{j'}$ system. The $O_A^{1'}$ line has a negligible intensity at zero field but is induced by a magnetic field along any direction. Again, two components are resolved with energies which are almost isotropic in the magnetic fields [Fig. 4(b)].

The data are very similar to those of the well-known singlet-triplet lines formed by some bound excitons in which a hole is trapped at an isoelectronic center and its orbital angular momentum is quenched by the axial local symmetry of the defect.[13] The remaining angular momentum of the exciton is the sum of the spins of the hole and the electron, giving a lower-energy (spin one) triplet state and a higher (spin zero) singlet state, typically split by an energy of the order of a meV. For those systems where the hole's angular momentum is strongly quenched, the triplet splits isotropically in a magnetic field, with energy changes

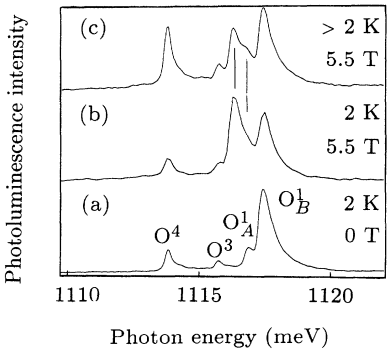

FIG. 3. (a) The O^j system recorded at 2 K using 200-mW laser excitation in a zero magnetic field. In (b) a field of 5.5 T has been applied along ⟨001⟩. O_B^1, O^3, and O^4 are not perturbed, but O_A^1 splits into two observable components which are flagged by the vertical lines. They are shown more clearly in (c), where an increased laser power of 400 mW has been used to raise the temperature slightly.

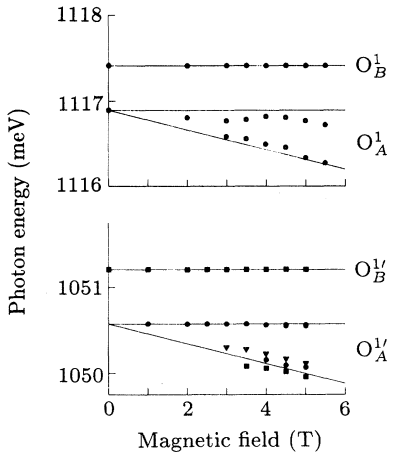

FIG. 4. (a) Variation of the O_B^1 and O_A^1 line energies with increasing magnetic field applied along the ⟨110⟩ direction. (b) Variation of the $O_B^{1'}$ and $O_A^{1'}$ line energies with increasing magnetic field. There is no variation of the energy of the $O_B^{1'}$ line up to 5 T. The datum points marked by the circles, squares, and triangles show the split $O_A^{1'}$ lines for the magnetic-field directions ⟨001⟩, ⟨111⟩, and ⟨110⟩, respectively. The lines are calculated using Eq. (3.1) with $g=2$ and $m_j=0$ and -1.

$$\Delta E = g\mu_B B m_s \tag{3.1}$$

where $m_s=0,\pm1$. The lines drawn on Fig. 4 show the expected energy shifts for $m_s=0$ and -1, assuming the pure spin value of $g=2$. The component with $m_s=+1$ would be masked by the O_B^1 transition.

The almost isotropic signals do not give any symmetry information about the defects, but do suggest that the hole is bound in an axial field so as to quench its orbital angular momentum.

IV. UNIAXIAL STRESS PERTURBATION STUDIES

A. O^j system

Figure 5 shows representative spectra for the O^j lines under ⟨001⟩, ⟨111⟩, and ⟨110⟩ compressions. In all stress directions the O^1, O^3, and O^4 lines move rigidly together, as shown by the energy plot in Fig. 6, and as is especially clear in the ⟨001⟩ spectra of Fig. 5(a). Since the strains do not couple directly to the spins of the particles, the near orthogonality of the spin singlet and triplet states forbids mixing of O_A^1 into O_B^1 under stress, in contrast to the effects of magnetic perturbations.

Under ⟨110⟩ stress the spectra recorded with electric vector **E** parallel to the stress **S** are independent of the direction of propagation of the luminescence, while the spectra recorded with **E** perpendicular to **S** do vary with the direction of **E** [Figs. 5(c) and 5(d)]. These are the characteristics of an electric-dipole transition.[14]

It is useful first to take an approximate overview of the data of Fig. 5. Under ⟨001⟩ stress the transitions split

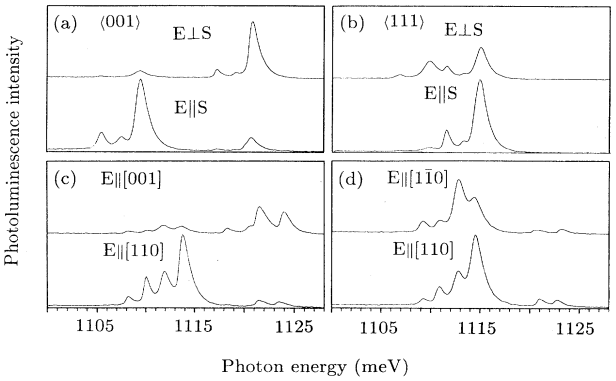

FIG. 5. The effects of uniaxial stresses on the O^j lines at 4.2 K under (a) 103-MPa ⟨001⟩ stress, (b) 312-MPa ⟨111⟩ stress, and (c) 155-MPa [110] stress for the [1$\bar{1}$0] viewing direction, and (d) 153-MPa [110] stress for the [001] viewing direction. The spectra have been recorded with the electric vector **E** parallel and perpendicular to the stress axis **S**.

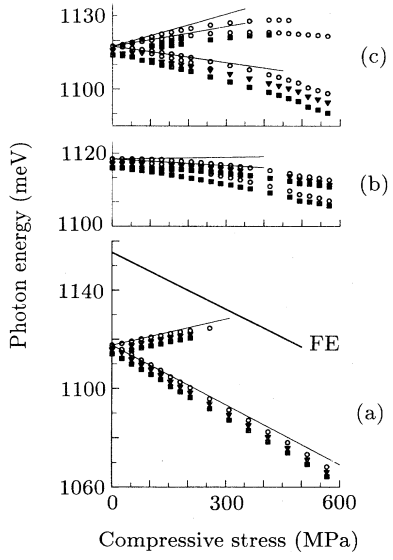

FIG. 6. Stress dependence, measured at 4.2 K, of the energies of the O^j lines under (a) ⟨001⟩, (b) ⟨111⟩, and (c) ⟨110⟩ compressions. The open circles, triangles, and squares show the stress-split components derived, respectively, from the O^1, O^3, and O^4 lines. The solid lines are least-squares fits of the theoretical expressions (Table I) to the data for the components derived from O_B^1. Under ⟨001⟩ stress the higher-energy components disappear at about 300 MPa. The stress dependence of the lowest-energy free-exciton state is shown by the broken line. In the fit using the tetragonal symmetry, the ⟨001⟩ fit is exactly as shown. For ⟨111⟩ stress only one line would be observed at the mean of the two shown, and for ⟨110⟩ stress the two high-energy components would be observed as one line at their mean.

into two components, with one almost completely polarized with **E** parallel to **S** and one polarized perpendicular to **S**. Ignoring the small splittings in ⟨111⟩ stress, only one component is observed with equal intensities in the **E**||**S** and **E**⊥**S** polarizations. Under [110] stress the splitting patterns are approximated by one transition seen with equal intensities when **E**||[110] and **E**||[1$\bar{1}$0], and a second transition seen with **E**||[001]. In this approximation the transition is exactly as is expected for the easily visualized case of an electric-dipole transition between nondegenerate orbitals at a tetragonal (⟨001⟩-oriented, point group D_{2d}) center with the dipole oriented along the main axis.[14] (Exactly the same results can be obtained for a transition between a nondegenerate and a triply degenerate state at a tetrahedral center,[15] but this case will be ruled out in Sec. V.)

The energies of the stress-split components (Fig. 6) all curve to lower energy, as expected if the excited state interacts with the higher-lying states which are known from luminescence-excitation spectroscopy.[7] Because the higher states are not accessible by low-temperature luminescence spectroscopy, we have little information on the interaction, and the nonlinearity will not be discussed here. This effectively limits the discussion to low stresses, where there is negligible interaction between states. To determine the linear part of the shift rates, a least-squares fit of a quadratic has been made to the measured energy of each stress-split component.

A nondegenerate orbital state at a tetragonal center is perturbed by the components of the stress tensor components s_{ij}, which are totally symmetric in the D_{2d} point group. These are, for the center which is oriented along [001], s_{zz} and $(s_{xx}+s_{yy})$, in terms of the crystal's cubic axes x, y, and z. The linear part of the change in energy of the optical transition can then be expressed in terms of two parameters A_1^t and A_2^t:[14]

$$\Delta E = A_1^t s_{zz} + A_2^t (s_{xx}+s_{yy}) . \tag{4.1}$$

A close fit to the linear shift of each stress-split component results when $A_1 \sim -80$ and $A_2 \sim 36$ meV/GPa, as described in the caption to Fig. 6.

The purpose of this approximate treatment is that it allows us to identify most of the stress response as deriving from an electron which is weakly bound on the center so that it maintains properties like those of an electron in the conduction-band minima. Silicon has conduction-band minima located near the ⟨001⟩ Brillouin-zone boundaries. Under [001] compression the [001] minima are lowered and the [100] and [010] minima are raised in energy, with a splitting of 92.5 meV/GPa.[16] For comparison, the linear splitting of the O^j lines is measured to be ~100 meV/GPa from Fig. 6(a). Similarly under ⟨111⟩ compression there is no splitting of the ⟨001⟩-oriented conduction-band minima, and the O^1 lines are not appreciably split.

We now refine the fit to include the minor splittings. Under [110] stress two higher-energy components are seen predominantly with **E**||[001]. This splitting is predicted if the symmetry of the center is slightly lower than D_{2d} (tetragonal class), and is C_{2v} (rhombic I class).[14] The

C_{2v} point group has the C_2 axis parallel to a ⟨001⟩ direction just as for the D_{2d} center. The polarization selection rules require the electric dipole of the transition to be along the C_2 axis (Table I), as expected, of course, from the tetragonal approximation. Small deviations in the polarizations between the theory and experiment are probably inaccuracies in the complete polarization of the data, and are ignored. For the center oriented with $C_2 \| [001]$, the perturbation of the transition is given by[14]

$$\Delta E = A_1 s_{zz} + A_2(s_{xx}+s_{yy}) + 2A_3 s_{xy} \ . \tag{4.2}$$

This equation is precisely that for the tetragonal center, Eq. (4.1), but with the additional term A_3, which can therefore be regarded, qualitatively, as measuring the deviation from tetragonal symmetry. The least-squares fit to the linear parts of the energy shifts yields the calculated shifts shown by the lines on Fig. 6, with

$$A_1 = -81 \text{ meV/GPa} \ , \quad A_2 = 36 \text{ meV/GPa} \ , \quad A_3 = \pm 8.5 \text{ meV/GPa} \ . \tag{4.3}$$

The mean error between the experimental values E and the fit f is $|E-f| = 2.8$ meV/GPA, compared to a mean of the $|E|$ of 32 meV/GPa. The sign of A_3 cannot be determined for this type of transition.

To summarize, the uniaxial stress data indicate that all the splitting of the O^j lines comes from the loosely bound electron, moving in an approximately tetragonal symmetry, but which shows evidence for a small reduction to rhombic I. The hole does not give an appreciable contribution to the stress splitting.

B. $O^{j'}$ system

Figure 7 shows the effect of the uniaxial stress on the $O^{j'}$ spectra. Figures 7(c) and 7(d) correspond to the two viewing directions, $[1\bar{1}0]$ and [001], respectively, for a [110] stress, and again establish the electric-dipole nature of the transitions. All three $O^{j'}$ lines behave very similar-

TABLE I. Predicted relative intensities of the stress-split components for an electric dipole parallel and perpendicular to the C_2 axis of a C_{2v} rhombic I center. Polarization data are shown for the electric vector **E** of the light relative to the stress axis **S** in the form **E**∥**S**:**E**⊥**S**. For [110] stress, the polarizations are shown for **E**∥[110]:∥[001]:∥$[1\bar{1}0]$. The shift rates of the components are given in terms of the parameters A_1, A_2, and A_3 defined in Eq. (4.2).

Stress axis	Shift rate	Electric-dipole axis ∥C_2	⊥C_2
⟨001⟩	A_2	0:1	2:1
	A_1	1:0	0:1
⟨111⟩	$(A_2+2A_2-2A_3)/3$	1:1	0:3
	$(A_1+2A_2+2A_3)/3$	1:1	4:1
[110]	A_2-A_3	0:0:1	0:0:1
	A_2+A_3	0:1:0	1:0:0
	$(A_1+A_2)/2$	2:0:2	1:2:1

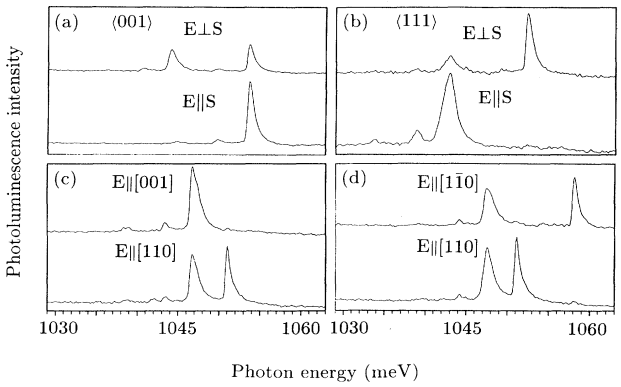

FIG. 7. The effects of uniaxial stresses on the $O^{j'}$ lines at 4.2 K under (a) 103-MPa ⟨001⟩ stress, (b) 312-MPa ⟨111⟩ stress, and (c) 1550-MPa [110] stress for the $[1\bar{1}0]$ viewing direction, and (d) 153-MPa [110] stress for the [001] viewing direction. The spectra have been recorded with the electric vector **E** parallel and perpendicular to the stress axis **S**.

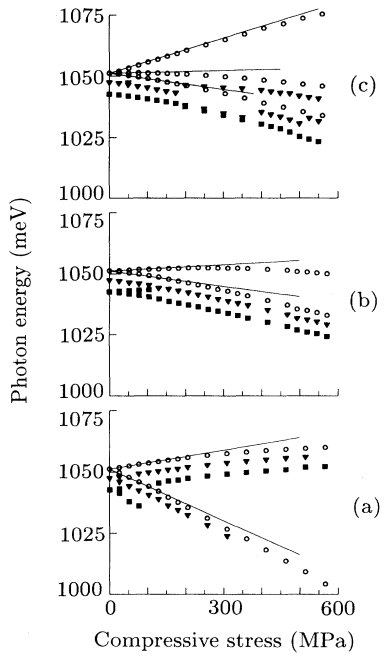

FIG. 8. Stress dependence, measured at 4.2 K, of the energies of the $O^{j'}$ lines under (a) ⟨001⟩, (b) ⟨111⟩, and (c) ⟨110⟩ compressions. The open circles, triangles, and squares show the stress-split components derived, respectively, from the O^1, O^3, and O^4 lines. The solid lines are least-squares fits of the theoretical expressions (Table I) to the data for the components derived from O_B^1. Note that, in contrast to the O^j system, under ⟨001⟩ stress the higher-energy components are stable to the highest stresses.

ly with the stress.

The numbers of stress split components for each stress axis and their intensities in the different polarizations establish the transitions as having their electric dipoles oriented along a $\langle 110 \rangle$ axis of a C_{2v}, rhombic I, center (Table I and Ref. 14).

The energies of the stress-split components are shown in Fig. 8 for stresses up to 600 MPa. Again, the lines are the least-squares fits of quadratic curves to the stress-split components derived from the highest-energy line $O^{j'}$. As for the O^j center, it is not profitable here to consider the nonlinearity in the shift rates. The least-squares fit to the linear parts of the shifts yields the lines on Fig. 8 with

$$A_1' = -70 \text{ meV/GPa}, \quad A_2' = 26 \text{ meV/GPa}, \quad A_3' = -22 \text{ meV/GPa}, \tag{4.4}$$

where the parameters are defined as in Eq. (4.2). The mean deviation $|E-f|$ between the experimental values E and the fit f is only1.3 meV/GPa, compared to a mean of the $|E|$ of 28.2 meV/GPa, confirming the assignment to a rhombic symmetry. The sign of A_3 is stated to be negative. This is valid if the optical transition is between states of irreducible representations A_1 and B_1 at the C_{2v} center, and the polarizations and shift rates in Table I are correct for this assignment. The same experimental data for the polarizations and shift rates would be obtained for a transition between A_1 and B_2 states, but with $A_3 = +22$ meV/GPa and with the sign of A_3 changed in Table I. These two types of transitions (which differ by having their electric dipoles normal to the two different reflection planes in the C_{2v} center) cannot be distinguished by experiment alone.

Again, the splitting under $\langle 001 \rangle$ stress of about 80 meV/GPa, with the shift rate of the upper component A_1 about half that of the lower component A_2, strongly implies that the splitting arises from the conduction-band splitting.[16] In terms of the bound-exciton model these results again suggest that the electron has properties derived from the conduction-band minima.

V. DISCUSSION

The effects of magnetic fields have been shown to leave most of the transitions in the O^j lines unperturbed (Sec. III). However, the O_A^1 line is split by the field, and, although one component is probably masked, the energies of the perturbed lines suggest that the O_A^1 line is from a triplet excited state formed by the spin pairing of the electron and hole. The energy separation to the singlet state (O_B^1) is 0.5 meV. This situation is typical of excitons bound to isoelectronic psuedodonor centers in silicon. The singlet-triplet energy separation is critically dependent on the overlap of the wave functions of the electron and hole, but typical values are 0.32 meV for the shallow 1138-meV transitions of the B_{71}^1 center,[17] and 1 meV for the slightly deeper 1045-meV transitions at a Li-related center.[18] The similar value for the O^j lines indicates that the electron and hole states have similar overlaps, and so they are bound at one defect. This rules out the suggestion that they are trapped on different defects (as in the donor-acceptor pair model[12]). The same arguments apply to the $O^{j'}$ system, where the singlet-triplet separation is ~ 0.6 meV.

Further confirmation of the orthodox triplet/singlet structure of the excited states comes from the relative intensities of the O_A and O_B lines. The transitions from the triplet and singlet states of excitons trapped at isoelectronic centers have relative transition probabilities I_t/I_s which are observed to follow a surprisingly uniform trend over three orders of magnitude when expressed in terms of the binding energy E of the exciton. (E is defined as the energy difference between the free exciton, 1155 meV, and the zero-phonon line.) The relationship can be partly justified in terms of the combinations of the valence-band maxima resulting from the low-symmetry field of the defect.[19] For a binding energy of 38 meV as for the O^j lines, the ratio is expected to be 0.05, and for the $O^{j'}$ lines (binding energy 103 meV) it is lowered to 0.01. It is difficult to measure a precise value for I_t/I_s for the O^j and $O^{j'}$ systems, given the broad optical components, but, allowing for the Boltzmann population in the triplet/singlet states, the relative transition probabilities are 0.06 ± 0.02 for the O^j lines and less than ~ 0.01 for $O^{j'}$, in reasonable agreement with the established empirical trend for isoelectronic centers.

For both the O^j and $O^{j'}$ systems, the magnetic data and the relative intensities at zero field are thus consistent with the holes of the bound excitons being bound at isoelectronic centers in a low symmetry which quenches the orbital angular momentum. The isoelectronic property excludes the possibility of a two-electron transition,[9] since this requires an extra electron in the ground state of the transition.

We turn next to the uniaxial stress data, taking first the O^j center. The effects of uniaxial stress derive primarily from a loosely bound electron (Sec. IV A). One result is that, despite the considerable stress response of the optical transition, there is no vibronic sideband: qualitatively, the electronic orbital contains too many atoms for there to be appreciable lattice relaxations caused by changes in that orbital. This situation is common, for example, when electrons are bound to shallow donors.[20] In Sec. IV, an approximate description was given for the stress response of the O^j system in terms of tetragonal symmetry, and it was noted that an alternative approximate description is as a tetrahedral center. It is useful to demonstrate that the tetrahedral assignment is not valid, so as to further confirm the low-symmetry nature of the center. In the model of a weakly bound electron, the six conduction-band minima would form A_1, E, and T_2 states in T_d symmetry. The A_1 state is not split by stresses. Under $\langle 100 \rangle$ stress the E state splits at two-thirds the rate of the conduction-band minima, and the T_2 state splits by an amount equal to the splitting of the minima.[21] In T_d symmetry the T_2 valley-orbit states would have to be the lowest in energy, as happens at the Li donor,[20] so that stresses along $\langle 001 \rangle$ would produce the observed splitting pattern. Thermalization between the split T_2 states is forbidden, at low stresses, since the split T_2 states correspond to the different conduction-band minima. Consequently an electron cannot deexcite

between these minima until their energy splitting is large enough that the valley-orbit phonon of 18 meV can be emitted: this effect produces the well-know hot and cold excitons familiar from work on free excitons[22] and some bound-exciton systems.[23] When the splitting exceeds 18 meV, the intensity of the luminescence from the hot exciton decreases very rapidly. Localization effects (which destroy the wave-vector selection rule) will lower the critical splitting required for loss of the high-energy component. At the O^j center, the high-energy component is readily observable under $\langle 001 \rangle$ stress until its splitting from the lower state is 30 meV (Fig. 6), considerably in excess of the figure likely for T_2 valley-orbit states.

The lack of thermalization is more readily explained by the low symmetry. In this case we would require one of the T_2 orbitals to be lowered in energy relative to the other two, as a result of a local strain along the $\langle 001 \rangle$ axis of the (D_{2d} or C_{2v}) defect. Under $\langle 001 \rangle$ stress we then expect the stress-split components to have constant intensities (assuming that the axis of the defect cannot be reoriented by the stress, in which case a very rapid loss of intensity is expected for the high-energy component). The intensity data therefore favor a low symmetry. A *compressive* stress derived from the main axis (say [001]) of the center and acting on the local lattice will lower two (z and $-z$) of the conduction-band minima. The loss of intensity in the high-energy component of O^1 which occurs at high stresses is probably caused by destabilization of the hot exciton into the cold free-exciton states, whose energy is shown by the broken line on Fig. 6(a). This explanation of the loss of the high-energy component is supported by the fact that, as shown below, the $O^{1'}$ transition involve very similar electron states to those of O^1 but does not lose luminescence when its splitting is by over 50 meV; the excited state is too deep to cross the conduction-band states with attainable stresses.

It is tempting to assign the nondegenerate orbital hole state, required to form the singlet/triplet structure (Sec. III) as another result of the local stress, since a large compressive [001] stress pulls the p_z state out of the valence-band maxima. This simple description works for some isoelectronic centers in silicon.[24] However, it is not valid here, since a pure p_z orbital would respond strongly to [001] stresses (at the rate of 45 meV/GPa, from the data of Ref. 16), and we have noted that the hole state is not perturbed by stresses at the O^j center (Sec. IV A). This lack of response is a surprising result, but is also found at other centers in silicon (e.g., the 789-meV transition at the C_i-O_i "C" center.[25]) While it is not understood, the lack of hole splitting excludes those models for the transitions which involve a free hole,[10,11] since the free hole responds strongly to uniaxial stresses (e.g., with a splitting of 45 meV/GPa under $\langle 001 \rangle$ stress[16]).

At the more deeply bound $O^{j'}$ center the symmetry is unambiguously rhombic I (Sec. IV B), and the splitting is again primarily determined by the electron. Consequently the parameters A_1' and A_2' are similar to A_1 and A_2 of O^j. The increased value of $|A_3|$ can be taken to indicate an increased sensitivity to the rhombic I symmetry of the defect. Since the coupling of the electrons to a shear stress is zero, the nonzero value of A_3 is not determined by the electron. The larger value at the $O^{j'}$ center suggests that the hole is more localized that at O^j, consistent with the deeper binding of the center.

The implication is that the energies of the O^j and $O^{j'}$ excited states differ primarily in the greater binding of the hole at $O^{j'}$. However, a major difference in the two centers is that the dipole moment is differently oriented, being parallel to the C_{2v} axis for O^j and perpendicular for $O^{j'}$ (Sec. IV). This difference is not understood, and as we noted for the O^j center, the structure of the hole state is not simply a combination of the valence-band maxima.

Of the four proposed models for the nature of the optical transitions, we have excluded all but the model of multiexcitons bound to isoelectronic centers. In this model only one line (O^1) would be observed at the O^j center with low excitation power, corresponding to the decay of one exciton bound to the center. With increasing power a second exciton may be bound before the first has decayed. All the published work[7,12] shows that the O^4 line increases relative to O^1 with increasing power, while the intensity of O^3 relative to O_B^1 is almost independent of the power. Figure 9 confirms this observation for the O^j lines, and demonstrates that under a $\langle 001 \rangle$ stress both the high- and low-energy components behave in the same way—the lifting of the degeneracy by the stress has no effect on the multiexciton creation. A different way of enhancing the O^4 line is by increasing the $\langle 001 \rangle$ stress under constant excitation power, until the high-energy component decreases. We have suggested that this is caused by destabilization of the higher-energy bound excitons, making more excitons available for capture into the lower-energy exciton states and increasing the intensity of O^4 (Fig. 10).

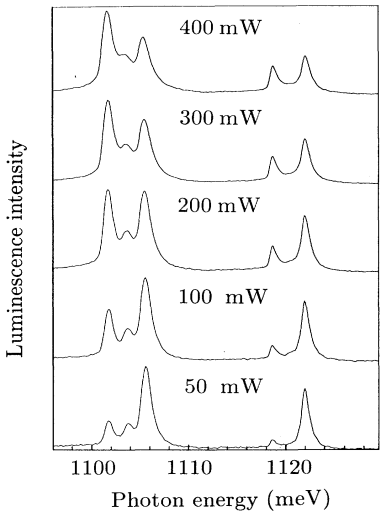

FIG. 9. Variation of the relative intensities of the O^j lines under $\langle 001 \rangle$ stress of 159 MPa with increasing excitation power. Spectra were obtained at 4.2 K using the 120-h annealed sample.

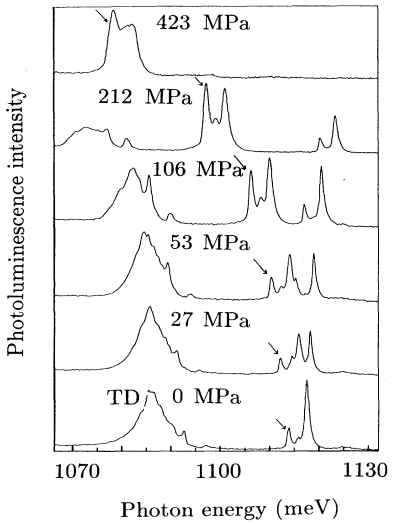

FIG. 10. Variation of the relative intensities of the O^j lines with increasing ⟨001⟩ stress. The feature labeled TD is produced by recombination of excitons at the thermal donors with the emission of one wave-vector-conserving phonon of 58 meV. The spectra were all obtained with 200-mW laser excitation at 4.2 K using a sample which had been annealed for 120 h. The increase in the low-energy component derived from O^4 (arrowed) is discussed in Sec. V.

The intensity data support the assignment of O^4 to the decay of a second bound exciton. Because the energy of the O^4 line is within 4 meV of that of O^1, the binding of both excitons is very similar, at about 38 meV, and we have to assume that the excitons have very similar properties. Under stress each exciton will then be perturbed identically. Since the O^4 transition occurs between the two-exciton state and the one-exciton state, the excited state will be perturbed by twice the ground-state perturbation. The optical transition will therefore be perturbed at the same rate as the single exciton, as observed. Note that the linewidth of O^4 is less than that of O^1 (Fig. 2). This is consistent with the two-exciton description of O^4 since the high-energy tail of O^1 has a shorter lifetime than the main peak (Sec. I), and multiexciton production favors the longer-lived centers.

The intensity of O^4 and its stress response are therefore consistent with its originating in a two-exciton state. The intensity behavior does not show strong evidence for O^3 involving a multibound exciton, or for the growth of an O^2 component under O^1. We recall that in order to quench the orbital angular momentum of the hole, it must be bound to an axial defect, and its orbital state is then nondegenerate. In terms of the shell model,[25] an orbitally nondegenerate hole state can only contain two holes, in a spin-paired nonparamagnetic state. A maximum of two bound excitons is then expected for a sufficiently axial center. This number is not affected by large stresses, as observed in Fig. 8, since the stresses do not lift the spin degeneracy. The spin pairing of the holes in the two-exciton state together with spin-paired electrons will result in a total spin for the two-exciton state of zero, and so a lack of magnetic perturbations, as observed for the O^4 and $O^{j'}$ lines (Sec. III). The same arguments follow for the $O^{j'}$ center.

Finally we note that the structure of the electronic state, derived from a pair of conduction-band minima, and the rhombic I symmetry of the centers are the same as for the thermal donors.[26] In our work, as in Refs. 7 and 8, the O^j and $O^{j'}$ systems appear to grow as the thermal donors are destroyed (Fig. 1). It is possible that they represent the neutral charge state of the next stage in the evolution of the thermal donors, similar to the way that the thermal donors themselves are a series of different aggregates but all with the same symmetry and electronic structure.

VI. SUMMARY

We have shown that the magnetic perturbations of the O^j and $O^{j'}$ centers establish that each has a weakly allowed transition which originates in a spin-triplet state, confirming the suggestion by Thewalt *et al.*[7] that the centers are isoelectronic with the lattice, and bind an exciton to produce the O^1 and $O^{1'}$ lines. The relative transition probabilities in the triplet and singlet components of O^1 and $O^{1'}$ further support this assignment. One important result from this conclusion is that the hole in the exciton is bound in a nondegenerate orbital state by the low-symmetry field at the defect, so that its orbital angular momentum is partially quenched. The effects of uniaxial stresses have been found to derive almost entirely from the electron component of the exciton, at both centers, and show that the electron is in a shallow, conduction-band-like state. With increasing exciton density in the crystal, whether produced by increasing the excitation power or by destabilizing some of the bound excitons by stress, one other component in the O^j and $O^{j'}$ centers increases in relative intensity, consistent with its involving a two-exciton excited state as proposed in Ref. 7. In contrast to Ref. 7, we have data for only two bound excitons, and this is expected to be the limit allowed by the shell model at a strongly axial center.

The data presented here have explicitly excluded three proposed models for the type of transitions occurring. The remaining model, involving multibound excitons, is confirmed, with strong evidence for two excitons being bound at the center. The electronic structure of both centers and their symmetry support the suggestion[7,8] that it has evolved from the thermal donors.

ACKNOWLEDGMENTS

L.J. thanks the Overseas Research Studentship award and King's College London for financial support. This work was carried out with funding from the Engineering and Physical Sciences Research Council. We thank M.L.W. Thewalt for extensive discussions.

*Permanent address: Department of Physics, University of Jaffna, Jaffna, Sri Lanka.

[1]A review of the thermal donor problem is given by H. Bender and J. Vanhellemont, in *Handbook of Semiconductors,* edited by S. Mahajan (Elsevier Science, Amsterdam, 1994), Vol. 3, pp. 1637–1753.

[2]R. C. Newman, in *Defects in Electronic Materials,* edited by M. Stavola, S. J. Pearton, and G. Davies, MRS Symposia Proceedings No. 104 (Materials Research Society, Pittsburgh, 1988), p. 25.

[3]G. Davies and R. C. Newman, in *Handbook on Semiconductors* (Ref. 1), pp. 1557–1635.

[4]M. Claybourn and R. C. Newman, Mater. Sci. Forum **38-41**, 613 (1989).

[5]A. G. Steele and M. L. W. Thewalt, Can. J. Phys. **67**, 268 (1989).

[6]W. Kürner, R. Sauer, A. Dörnen, and K. Thonke, Phys. Rev. B **39**, 327 (1989).

[7]M. L. W. Thewalt, A. G. Steele, S. P. Watkins, and E. C. Lightowlers, Phys. Rev. Lett. **57**, 1939 (1986).

[8]A. G. Steele, M. L. W. Thewalt, and S. P. Watkins, Solid State Commun. **63**, 81 (1987).

[9]B. J. Heijmink Liesert, T. Gregorkiewicz, and A. J. Ammerlaan, Phys. Rev. B **47**, 7005 (1993).

[10]J. Weber and H. J. Queisser, in *Oxygen, Carbon, Hydrogen and Nitrogen in Crystalline Silicon,* edited by J. W. Corbett, J. C. Mikkelsen, Jr., S. J. Pearton, and S. J. Pennycook, MRS Symposia Proceedings No. 59 (Materials Research Society, Pittsburgh, 1986), p. 147.

[11]J. Weber, K. Köhler, F. J. Stützler, and H. J. Queisser, in *Defects in Semiconductors, 1986,* edited by H. J. Von Bardeleben (Materials Science Forum, Switzerland, 1987), p. 979.

[12]A. Dörnen and A. Hangleiter, in *Defects in Semiconductors 1986,* edited by H. J. Von Bardeleben (Materials Science Forum, Switzerland, 1987), p. 967.

[13]A general discussion is given by P. J. Dean and D. C. Herbert, in *Excitons,* edited by K. Cho, Topics in Current Physics Vol. 14 (Springer-Verlag, Berlin, 1979), p. 55; a specific application to silicon is given by G. Davies, J. Phys. C **17**, 6331 (1984).

[14]A. A. Kaplyanskii, Opt. Spectrosc. **16**, 329 (1964).

[15]A. A. Kaplyanskii, Opt. Spectrosc. **16**, 557 (1964).

[16]L. D. Laude, F. H. Pollack, and M. Cardona, Phys. Rev. B **3**, 2623 (1971).

[17]A. S. Kaminskii, E. V. Lavrov, V. A. Karasyuk, and M. W. L. Thewalt, Phys. Rev. B **50**, 7338 (1994).

[18]G. Davies, L. T. Canham, and E. C. Lightowlers, J. Phys. C **17**, L173 (1984).

[19]G. Davies, Phys. Rev. B **51**, 13 783 (1995).

[20]R. L. Aggarwal, P. Fisher, V. Mourzine, and A. K. Ramdas, Phys. Rev. **138**, A882 (1965).

[21]D. K. Wilson and F. Feher, Phys. Rev. **124**, 1068 (1961).

[22]V. D. Kulakovskii,I. B. Levinson, and V. B. Timofeev, Fiz. Tverd. Tela (Leningrad) **20**, 399 (1978) [Sov. Phys. Solid State **20**, 230 (1978)].

[23]Z. Ciechanowska, G. Davies, and E. C. Lightowlers, Solid State Commun. **49**, 427 (1984).

[24]G. Davies, Physica T **54**, 7 (1994).

[25]M. W. L. Thewalt, in *Excitons,* edited by E. I. Rashba and M. D. Sturge (North-Holland, Amsterdam, 1982), p. 393.

[26]M. Stavola, K. M. Lee, J. C. Nabity, P. E. Freeland, and L. C. Kimerling, Phys. Rev. Lett. **54**, 2639 (1985).